

MICROMECHANICAL INVESTIGATION OF SOIL PLASTICITY USING A DISCRETE MODEL OF POLYGONAL PARTICLES

F. Alonso-Marroquin and Hans B. Mühlhaus

ESSCC, The University of Queensland, Sta Lucia Qld 4068, Australia

Hans J. Herrmann

IfB, HIF E.11, ETH Hönggerberg CH 8093 Zürich, Switzerland

ABSTRACT : The mechanical behavior of soils has been traditionally described using continuum-mechanics-based models. These are empirical relations based on laboratory tests of soil specimens. The investigation of the soils at the grain scale using discrete element models has become possible in recent years. These models have provided valuable understanding of many micromechanical aspects of soil deformation. The aim of this work is to draw together these two approaches in the investigation of the plastic deformation of non-cohesive soils. A simple discrete element model has been used to evaluate the effect of anisotropy, force chains, and sliding contacts on different aspects of soil plasticity: dilatancy, shear bands, ratcheting, etc. The discussion of these aspects raises important questions such as the width of shear bands, the origin of the stress-dilatancy relation, and the existence of a purely elastic regime in the deformation of granular materials.

KEYWORDS: (Granular materials, incremental response, ratcheting, fabric, anisotropy).

1. INTRODUCTION

The 1960s was significant for the development of soil mechanics and, in particular, the constitutive models for soils. Prior to this decade, soil mechanics was confined to linear elastic theory and the Mohr-Coulomb failure criterion. An important advance in the scope of soil plasticity occurred after the pioneering work of Roscoe and his coworkers in Cambridge, which led to the basic principles of the Critical State Theory [1; 2]. In an attempt to cover further aspects of cyclic soil behavior, subsequent developments have given rise to a great number of constitutive models [3,4]. These advances were consolidated in two different trains of thought: The first one is the so-called black box approach, in which the constitutive relation is derived exploiting mathematical symmetries and representation theorems [5; 6]. The main advantage of this approach is that it offers a rigorous mathematical framework for the development of the tensor structure of constitutive relationships. The other train of thought is the micromechanical approach [7]. Micromechanical models are useful to identify physically relevant tensorial relations, to gain insight into the significance of material parameters, and to investigate the interconnection between phenomena occurring at the grain scale and bulk behavior.

The development of micromechanical constitutive models has been specially motivated by recent investigations on granular materials at grain scale [8]. Numerical and laboratory experiments show that stress in granular materials is transmitted through a heterogeneous contact network with broad force distribution [9]. This broadness leads in turns to a considerable number of sliding contacts. Under small deviatoric loads, an initially isotropic packing develops an anisotropic contact network because new contacts are created along the loading direction, while some contacts are lost perpendicular to it. Anisotropy is also observed in the subnetwork of the sliding contacts, because

some contact leave the sliding condition under slight deviatoric loading. Geometrical anisotropy leads to an anisotropic response of the granular assembly. The effect of anisotropy of the contact network on the anisotropic elasticity and the plasticity has been investigated by the introduction of fabric tensors, measuring the distribution of the orientation of the contacts [10; 11; 12]. This is a review of our recent work on the investigation of the dynamics of contact network and its effect on the overall response of granular media.

Granular samples are represented by assemblies of polygons generated by Voronoi tessellation (see Figure 1). The interparticle forces include elasticity, viscous damping and friction with sliding condition. The ratio between the tangential and normal contact stiffnesses is $k_t/k_n = 0.33$, and the friction coefficient is $\mu = 0.25$. Initially, the polygonal particles fill the plane with no overlaps and no gaps. This kind of plain tessellation resembles in some aspects the geometry of fragmented rocks, dry masonry walls or marble [12]. In Section 2 we investigate the micro-structure of the contact network at the shear band formation. In Section 3 we discuss the incremental plastic response of the contact network and its relation with the induced anisotropy in the subnetwork of sliding contacts. In Section 4 we introduce the granular ratcheting, as the response of the contact network when they are subjected to load-unload stress cycles.

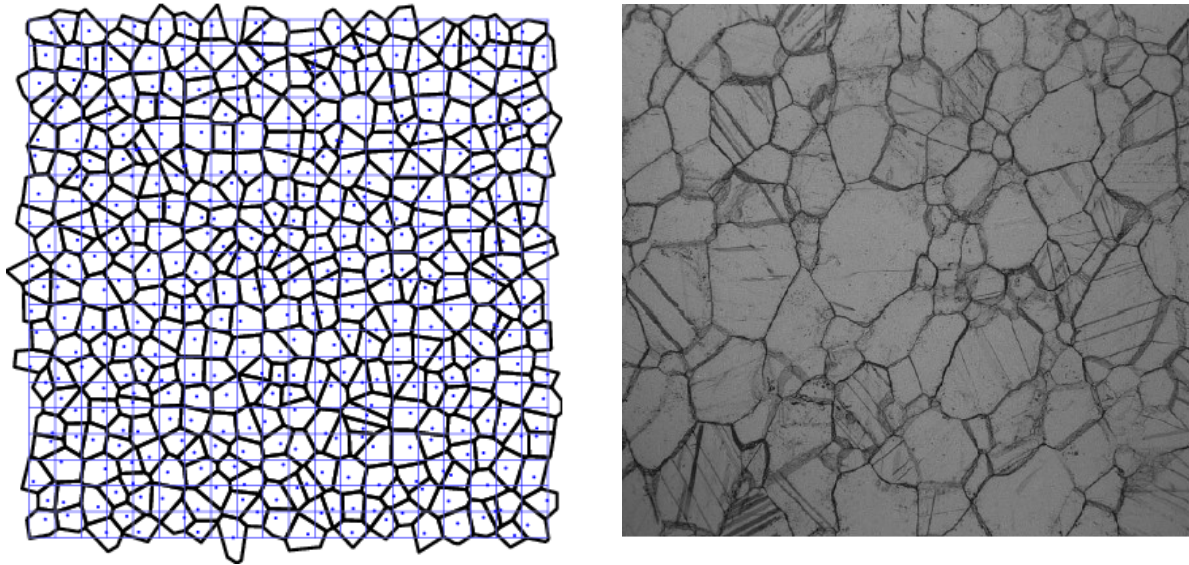


Fig. 1 Left: Voronoi construction used to generate the convex polygons. The dots indicate the point used in the tessellation. Periodic boundary conditions were used. Right: Typical texture of marble. (Courtesy of Royer-Carfagni [13])

2. SHEAR BAND FORMATION

Strain localization in form of shear bands is ubiquitous in geomaterials. For example, in laboratory tests with soil specimens [14] , and in the boundaries between two tectonic plates [15]. The incorporation of the characteristic width in shear bands in the continuum models has special significance from the computational point of view, because it resolves the mesh-dependency problems in the Finite Element simulations [16; 17; 18]. In experimental tests, the presence of shear bands is very sensitive to the boundary conditions. In our simulations we chose them in order to mimic the experimental tests under plane strain conditions: First, a confining pressure is applied to the sample through a flexible membrane. Then, two horizontal walls at the top and bottom of the packing are used to apply vertical loading with constant velocity. The details of the construction of such floppy boundary can be found elsewhere [19]. The deformation of the assembly involves creation and loss of contacts as well as restructuring by means of rolling and sliding contacts. These changes imply a

continuous variation of the stress-strain relation and a change of the void ratio during load. From the principal values of the average of the stress tensor, one can define the mean normal stress $p = (\sigma_1 + \sigma_2)/2$ and the deviatoric stress $q = (\sigma_1 - \sigma_2)/2$. The axial strain is calculated as $\epsilon_1 = \Delta H/H_0$, where H is the height of the sample. The volumetric strain is given by $e = \Delta A/A_0$.

The dependence of the deviatoric stress and the volumetric strain on the axial strain are shown in Fig. 2 for different confining pressures. A continuous decrease of the initial slope of the stress-strain curve is observed. Loading rearranges the contact network by means of sliding contacts, which in turn reduces the stiffness of the material. The initial compaction turns gradually to dilatancy. This transition is caused by loss of contacts perpendicular to the load direction, allowing the contact network to rearrange itself and inducing large plastic deformations. Near failure, the amount of plastic deformation is much larger than the elastic one. This considerably reduces the stiffness with respect to its initial value and makes the sample potentially unstable. Plastic deformation by means of sliding contacts turns out to be a precursor mechanism of strain localizations. The frictional dissipation is uniformly distributed at the beginning of the load and it tends progressively to localize in thin layers, which ends up with the shear band formation [20]. Near failure, the orientational distribution of sliding contacts has its maximal value between the Mohr-Coulomb angle and the Roscoe angle, but rather closer to the former [12]. The shear band is given by a 6 – 8 grain diameters thick layer where the frictional dissipation is more intense than on the average.

The characteristic width of the shear of the band can be associated to the propagation of stress inside the grains. The principal components of the stress

tensor averaged over each particle are represented in Fig. 2 by a cross. The length of the lines represents how large the components are. At the beginning of the loading, the major principal stress is almost parallel to the load direction, forming column-like structures which are called force chains. At failure these chains start buckling. The buckled chains gradually create force loops which concentrate as shear bands. The size of such loops corresponds to the shear band width, and it depends only on the grain diameter. Buckling of each force chain involves rolling between the grains belonging to it, a feature that has been used to provide a theoretical explanation of the finite width of shear bands [21].

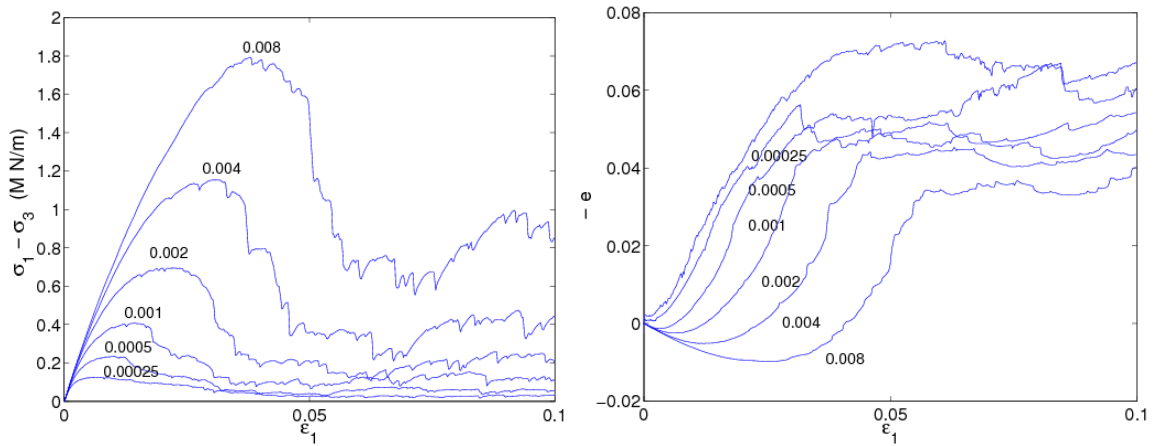
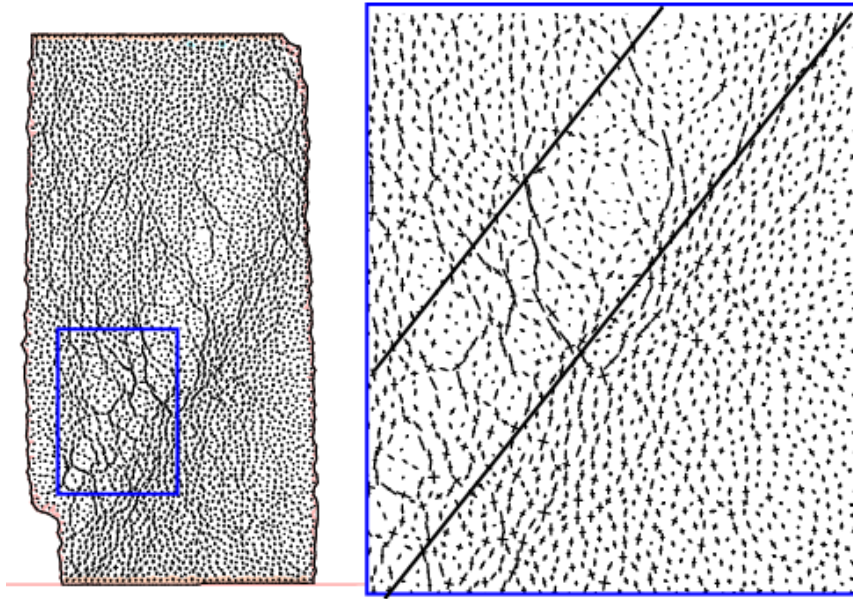


Fig. 2 Top left: Principal stress directions of the grains after failure ($\epsilon_1 = 0.07$); the confining pressure is $p_0 = 0.001k_1$. Top right: Detail of the stress in the shear band. Bottom: Deviatoric stress and volumetric strain versus axial strain for different values of p/k_n , where p is the lateral pressure. $e > 0$ represent compression of the sample.

3. INCREMENTAL RESPONSE

An important future application of particle based models is to use them as a virtual laboratory, where samples with relative large number of particles are used to construct the constitutive relations. They are to be given in terms of incremental relations, which can be used in the Finite Element Codes. The method we use to calculate the strain response is the same as used in sand experiments [22]. It was introduced by Bardet [23] in the calculation of the incremental response using discrete element methods. We denote the incremental strain as $d\boldsymbol{\varepsilon} = (de, d\gamma)$, being e and γ the volumetric and shear components. The stress is represented by the vector $\boldsymbol{\sigma} = (p, q)$, where p and q are the pressure and shear stress. Starting from $\boldsymbol{\sigma}$, the sample is loaded to $\boldsymbol{\sigma} + d\boldsymbol{\sigma}$ and the strain increment $d\boldsymbol{\varepsilon}$ is calculated. Then the sample is unloaded to $\boldsymbol{\sigma}$ and one finds a remaining strain $d\boldsymbol{\varepsilon}_p$, which corresponds to the plastic incremental strain. This procedure is implemented on different clones of the same sample, choosing different stress directions and the same stress amplitude in each one of them. We assume that the strain response after a reversal loading is completely elastic. Numerical simulations show that this assumption is not strictly true, because sliding contacts are always observed during the unload path [24; 25]. However, for stress amplitudes of $|d\boldsymbol{\sigma}| < 0.001p$ the plastic deformation during the reversal stress path is less than 1% of the corresponding value of the elastic response. Within this margin of error, the difference $d\boldsymbol{\varepsilon}_e = d\boldsymbol{\varepsilon} - d\boldsymbol{\varepsilon}_p$ can be taken as the elastic component of the strain.

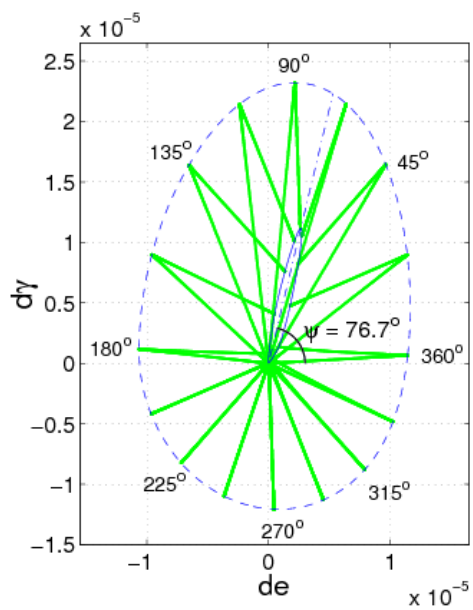
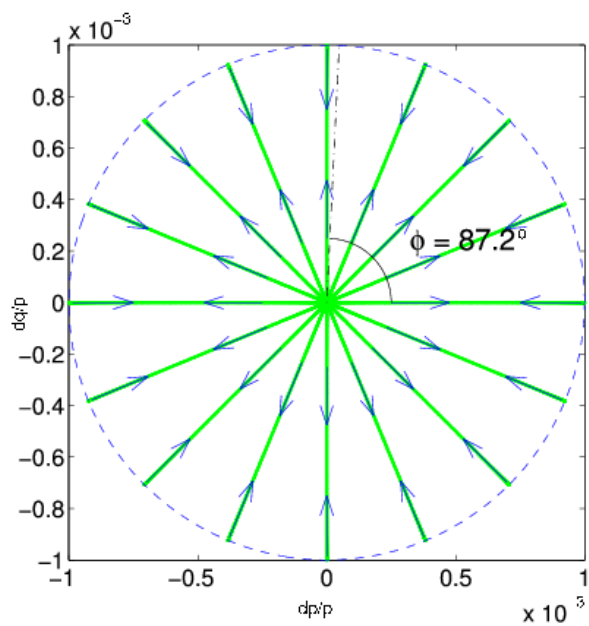


Fig. 3 Stress - strain relation resulting from the load - unload test. Grey solid lines are the paths in the stress and strain spaces. Grey dash-dotted lines represent the yield direction (top) and the flow direction (bottom). Dashed line shows the strain envelope response and the solid line is the plastic envelope response.

Fig. 3 shows the load-unload stress paths and the corresponding strain response when an initial stress state with $\sigma_1 = 1.25 \times 10^{-3}k_n$ and $\sigma_3 = 0.75 \times 10^{-3}k_n$ is chosen. The end of the load paths in the stress space maps into a strain envelope response $d\epsilon(\theta)$ in the strain space. Likewise, the end of the unload paths maps into a plastic envelope response $d\epsilon_p(\theta)$. This envelope consists of a very thin ellipse, nearly a straight line, which confirms the unidirectional aspect of the irreversible response predicted by the elastoplasticity theory [26]. The yield direction φ can be found from this response, as the direction in the stress space where the plastic response is maximal. In this example, this is around $\varphi = 87.2^\circ$. The flow direction ψ is given by the direction of the maximal plastic response in the strain space, which is around 76.7° . The fact that these directions do not agree reflects a non-associated flow rule, which is also observed in experiments on realistic soils [22]. From numerical simulations of packings of disks, Bardet concluded also that a non-associated flow rule describes satisfactorily the incremental response [23]. This conclusion is also supported by several experimental tests on plane strain deformation [26; 27; 2]. Both numerical and experimental results show clearly deviations from the normality condition. This is connected to the fact that any load involves sliding contacts so that the elastic regime is vanishing small but not a finite domain as the Classical Elastoplasticity establishes [28]. Recent numerical simulations of three dimensional packings of spheres contradict not only the normality postulate [29], but also the unidirectionality of the flow rule [30], leading also to

the conclusion that a profound modification of the elastoplasticity theory is required [31].

The elastic part of the incremental response is described using two Young moduli and two Poisson ratios[12]. This response can be characterized by introducing fabric coefficients, measuring the anisotropy of the contact network [12; 10]. The evolution of the fabric coefficients during loading is different from the observed evolution in loose granular packings. This is due to the fact that we start with a polygonal packing with zero porosity, where the force distribution is unusually narrow [12]. This is not typical in most granular materials where the force distribution is rather heterogeneous [9]. In dense polygonal packings with finite porosity [32] and disks assemblies, [10; 33] small loads open weak contacts and hence induce a smooth transition to the anisotropy for small deviatoric loads. In all cases, the evolution equation of the fabric coefficients in terms of the deformation history of the granular assembly is an open issue [34].

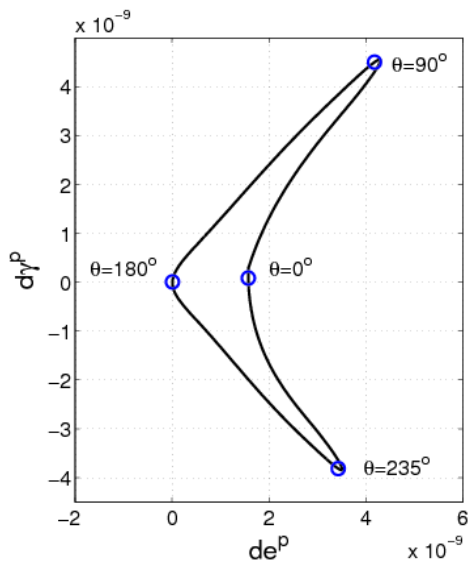
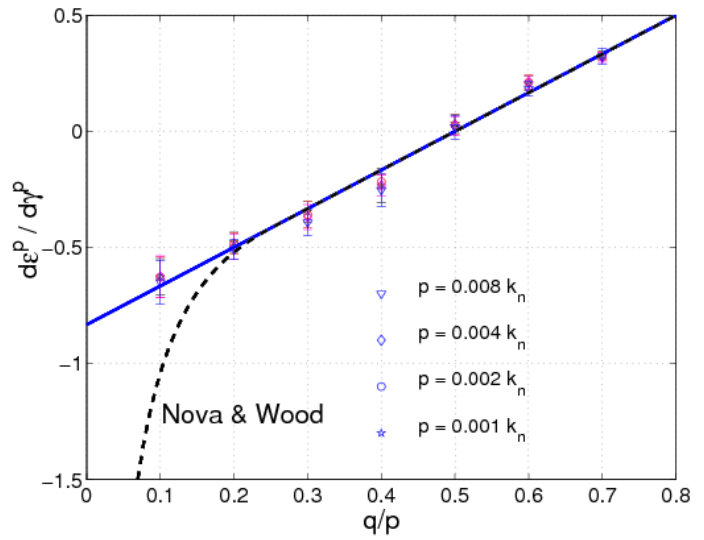


Fig. 4 Left: dilatancy versus the stress ratio. The solid curve represents a linear fit; The dashed curve the relation given by the Nova & Wood model. Right: plastic envelope response resulting from isotropically

compressed samples with a pressure $p = 0.001k_n$.

Apart from the unidirectionality of the flow rule, we find that dilatancy $d = -de_p/dy_p$ and the stress ratio $\eta = q/p$ are related by simple linear relation $d = c(\eta - M)$ (Fig. 4). This relation is not only supported by experiments, but also it has been one of the fundamental issues in modeling the stress-strain behavior of soils. However we have to notice that the micromechanical explanation of such a simple stress-dilatancy relationship has remained elusive. Although we cannot give a definitive answer to this question, a physical explanation would be that the granular sample behaves like a strange fluid that obeys this stress-dilatancy relation as an internal kinematical constraint [35]. This constraint becomes apparent near failure, where the plastic deformation dominates, and it could be seen as the counterpart of the well-known incompressibility condition of fluids. In this context we should address to the existing correlation between the mean orientation of the sliding contacts and the plastic flow direction [12]. This correlation suggests that this internal constraint can be micromechanically interpreted from the induced anisotropy of the subnetwork of the sliding contacts. In the limit of small deviatoric load, the kinematic constrain is not longer valid because elastic deformation dominates. However, we report some additional connections between stress-dilatancy relationship and the induced anisotropy in the subnetwork of sliding contacts. Under extremely small deviatoric loads, some contacts depart from the sliding condition, leading in turn to anisotropy in the subnetwork of the sliding contacts. The effect of this anisotropy in the plastic response becomes evident when we get the plastic envelope response of an isotropically compressed sample, see Fig. 4. Unexpectedly, the unidirectionality of the plastic deformations breaks down, because small deviatoric loads lead to deviatoric plastic deformations. This

surprising effect contradicts the isotropic regimen postulated in several constitutive models [27].

4. GRANULAR RATCHETING

In this last section we introduce a long time response of granular materials under cyclic loading, which is still under discussion in the scientific and engineering community. This effect is known as granular ratcheting, and it refers the constant accumulation of permanent deformation per cycle, when the granular sample is subjected to load-unload stress cycles with extremely small loading amplitudes. Although there is wide experimental evidence about accumulation of permanent deformation under cyclic loading [36], it is not clear whether this effect remains for loading amplitudes below the critical state, or there is a certain regime where the material behaves perfectly irreversible [27; 37; 38]. It is still also not clearly understood how sliding, crushing and wearing of the grains affect the accumulation of plastic deformation with the number of cycles [39; 40; 41; 36]. Here we present numerical evidence of this ratcheting effect for small loading amplitudes on assemblies of densely packed polygons. This can be detected at the micromechanical level by a ratchetlike behavior at the contacts. This effect excludes the existence of the rather questionable finite elastic regime of noncohesive granular materials.

We use samples with volume fractions lower than one. First, the polygons are placed randomly inside a rectangular frame consisting of four walls. Then, a gravitational field is applied and the sample is allowed to consolidate. The external load is imposed by applying a force $\sigma_1 H$ and $\sigma_2 W$ on the horizontal and vertical walls, respectively. Here σ_1 and σ_2 are the vertical and horizontal stresses. H and W are the height and the width of the sample. Next, the sample is isotropically compressed until the pressure p_0 is reached. When the velocity of

the polygons vanishes gravity is switched off. Then, the vertical stress $\sigma_1 = p_0$ is kept constant and horizontal stress is modulated as $\sigma_2 = p_0 + \Delta\sigma[1 - \cos(\pi t/t_0)]/2$. Part (a) of Fig. 5 shows the relation between the stress $q = (\sigma_1 - \sigma_2)/2$ and the shear strain γ in the case of a loading amplitude $\Delta\sigma = 0.424p_0$. This relation consists of open hysteresis loops which narrow as consecutive load-unload cycles are applied. This hysteresis produces an accumulation of strain with the number of cycles which is represented by γ_N in the part (b) of Fig 5. We observe that γ_N consists of short time regimes, with rapid accumulation of plastic strain, and long time ratcheting regimes, with a constant accumulation rate of plastic strain of around 2.4×10^{-6} per cycle. The relation between the stress and the volume fraction is shown in part (c) of Fig. 5. This consists of asymmetric compaction-dilation cycles leading to compact during the cyclic loading. This compaction is shown in part (d) of the Fig. 5. We observe a slow variation of the volume fraction during the ratcheting regime, and a rapid compaction during the the transition between two ratcheting regimes, whereas the slope of γ_N shows no dependency on the compaction level of the sample. The evolution of the volume ratio seems to be rather sensitive to the initial random structure of the polygons. Even so we found that after 8×10^3 cycles the volume fraction still slowly increases in all the samples, without reaching the saturation level.

By following the evolution of the contact network one can explain this particular behavior. Even under isotropic compression, the strong heterogeneities of the force network produce a considerable amount of contacts reaching the sliding condition. Those sliding contacts carry most of the irreversible deformation of the granular assembly during the cyclic loading. Opening and closure of contacts are quite rare events, and the coordination number of the packing

keeps it approximately its initial value 4.2 ± 0.08 in all the simulations. After certain loading cycles the contact forces reach the quasiperiodic behavior. In this regime, a fraction of the contacts reaches almost periodically the sliding condition. The load-unload asymmetry of the contact force loops makes the contacts slip the same amount and in the same direction during each loading cycle.

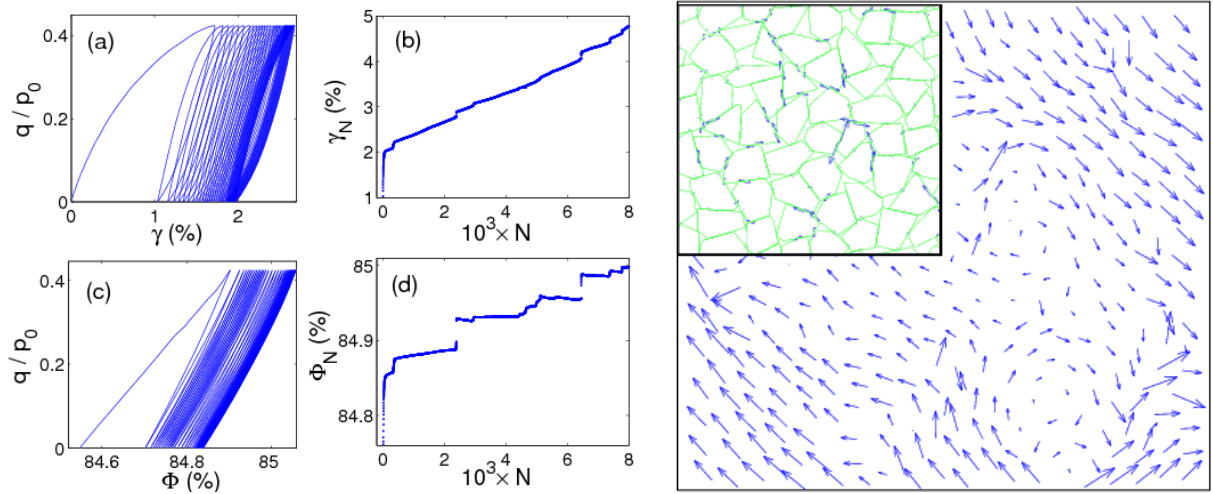


Fig. 5 Top: (a) Deviatoric stress versus shear strain in the first 40 cycles. (b) permanent (plastic) strain γ_N after N cycles versus the number of cycles. (c) stress against the volume fraction in the first 40 cycles. (d) volume fraction Φ_N after N cycles versus number of cycles. Bottom: displacement field after one cycle in the ratcheting regime. Inset: Permanent deformation per cycle at the contacts.

When the ratcheting regime is reached, each particle within the packing has a certain displacement and accumulates the same rotation for each cycle. It is of great interest to study the patterns created by the rotational and displacement field of all the grains. Slip zones, rotational bearings and vertical structures persist during the long time of a ratcheting regime [25; 42]. These structures are concentrated in shear bands, as shown the Figure 5. Recently it has been shown that these rotational patterns promote a strong reduction of strength and

frictional dissipation in shear cells [12]. They suggest also a characteristic mesoscopic scale in granular materials, which is required to connect their macroscopic behavior to the microscale. It is an open question how to introduce such rotational modes in the continuum, which certainly require an interconnection between the grain scale, the mesoscale of few grains, and the macroscopic scale of the bulk material.

5. CONCLUSIONS

A discrete element model of polygonal particles has been used to investigate the plastic deformation in non-cohesive granular materials. The response of the discrete model reproduces three important features of soil deformation: (1) The unidirectionality of the plastic strain response, (2) shear bands, and (3) the stress-dilatancy relation. Comparing the strain response to the anisotropy induced by loading in the contact network, we conclude that the elastoplastic response of granular materials can be described by using two set of fabric variables. The first set connects the elastic response to the anisotropy of the contact network. The second set of coefficients, measuring the anisotropy induced by loading in the subnetwork of sliding contacts, can be used to describe the micromechanics of the plastic deformation of the granular materials. Anisotropy plays also an important role in the shear band formation. Strain localization appears a mechanism of buckling of stress columns which gradually concentrate in layers which end up with the creation of the shear bands. The width of such shear bands is related to the characteristic length of the buckled columns and it depends only on the grain diameter.

Shear bands can be seen as the asymptotic response of granular materials for large monotonic plastic deformations. In the case of cyclic loading we have

reported on the existence of an asymptotic response for large number of cycles. This is the so-called granular ratcheting, which appears under cyclic loading with extremely small loading amplitudes. Ratcheting is characterized by a constant accumulation of plastic deformation with the number of cycles, resulting from a ratchet-like deformation at the sliding contacts.

The spatial distribution of such ratchets is not random, but their appear to be correlated in form of slip

bands. The displacement and rotational field of the individual particles are spatially correlated in terms of vorticity cells and rotational bearings. Such rotational patterns promote a strong reduction of frictional dissipation in shear cells, a feature that addresses important issues of soils mechanics, such as the principle of minimal energy dissipation for shear bands [43], the necessity of rotational degrees in the continuum description of granular media [44], and the long standing heat flow paradox of earthquakes mechanics [45]. With the recent advances in computational modelling, the push to investigate these issues on the basis of simulation will represent an important part of geotechnical and rock mechanics applications. One crucial issue in such modeling involves the use of multiscale approach [46], where the micromechanics of grain contact, along with the dynamics of mesoscopic patterns and the constitutive equations of the bulk materials, need to be treated simultaneously.

F. Alonso-Marroquin is the recipient of an Australian Research Council Postdoctoral Fellowship (project number DP0772409), and acknowledges the support of the ALERT Geomaterials Prize 2006.

Correspondence: fernando@esscc.uq.edu.au

6. REFERENCES

1. K. H. Roscoe and J. B. Burland. On the generalized stress-strain behavior of 'wet' clay. In *Engineering Plasticity*, Cambridge, Cambridge University Press, (1968), 535–609.
2. D. M. Wood. *Soil behaviour and critical state soil mechanics*. ISBN: 0-521-33782-8, Cambridge, 1990.
3. G. Gudehus, F. Darve, and I. Vardoulakis. *Constitutive Relations of soils*. Balkema, Rotterdam, 1984.
4. R. Scott. Constitutive relations for soils: Present and future. In *Constitutive Equations for Granular Noncohesive Soils*, Balkema, (1988), 723–726.
5. D. Kolymbas. *Modern Approaches to Plasticity*. Elsevier, 1993.
6. R. Chambon, J. Desrues, W. Hammad, and R. Charlier. CLoE, a new rate type constitutive model for geomaterials. Theoretical basis and implementation. *Int. J. Anal. Meth. Geomech.*, 18, (1994) 253–278.
7. A. Tordesillas, S. D. C. Walsh, and B. S. Gardiner. Bridging the length scales: Micromechanics of granular media. *BIT Numerical Mathematics*, 44(3), (2004), 539–556.
8. M. E. Cates, J. P. Wittmer, J.-P. Bouchaud, and P. Claudin. Jamming, force chains, and fragile matter. *Phys. Rev. Lett.*, 81(9), (1998), 1841–1844.
9. F. Radjai, M. Jean, J. J. Moreau, and S. Roux. Force distribution in dense two-dimensional granular systems. *Phys. Rev. Lett.*, 77(2), (1996), 274.
- 10.10. S. Luding. Micro-macro transition for anisotropic, frictional granular packings. *Int. J. Sol. Struct.*, 41, (2004), 5821–5836.
11. M. Madadi, O. Tsoungui, M. Latzel, and S. Luding. On the fabric tensor of polydisperse granular media in 2d. *Int. J. Sol. Struct.*, 41(9-10), (2004), 2563–2580.

12. F. Alonso-Marroquin, S. Luding, H.J. Herrmann, and I. Vardoulakis. Role of the anisotropy in the elastoplastic response of a polygonal packing. *Phys. Rev. E*, 71, (2005), 051304.
13. G. Royer-Carfagni and W. Salvatore. The characterization of marble by cyclic compression loading: experimental results. *Mech. Cohes.-Frict. Mater.*, 5, (2000), 535–563.
14. J. Desrues. Localisation de la deformation plastique dans les materieux granulaires. PhD thesis, University of Grenoble, 1984.
15. P. Mora and D. Place. The weakness of earthquake faults. *Geophys. Res. Lett.*, 26, (1999), 123–126.
16. H.-B. Mühlhaus and I. Vardoulakis. The thickness of shear bands in granular materials. *Geotechnique*, 37, (1987), 271–283.
17. P. Papanastasiou and I. Vardoulakis. Numerical treatment of progressive localization in relation to borehole instability. *Int. J. Num. Anal. Meth. Geomechanics*, 16(6), (1992), 389–424.
18. J. Techman and E. Bauer. Numerical simulation of shear band formation with a polar hypoplastic constitutive model. *Computers and Geotechnics*, 19(3), (1996), 221–244.
19. F. Alonso-Marroquin and H. J. Herrmann. Calculation of the incremental stress-strain relation of a polygonal packing. *Phys. Rev. E*, 66, (2002), 021301.
20. F. Alonso-Marroquin. Micromechanical investigation of soil deformation: Incremental Response and granular Ratcheting. PhD thesis, University of Stuttgart, 2004. Logos Verlag Berlin ISBN 3-8325-0560-1.
21. M. Satake. Finite difference approach to the shear band formation from the viewpoint of particle column buckling. In *Thirteenth Southeast Asian Geotechnical Conference*, (1998), 815–818.

- 22.H. B. Poorooshasb, I. Holubec, and A. N. Sherbourne. Yielding and flow of sand in triaxial compression. *Can. Geotech. J.*, 4(4), (1967), 277–398.
- 23.J. P. Bardet. Numerical simulations of the incremental responses of idealized granular materials. *Int. J. Plasticity*, 10, (1994), 879–908.
- 24.F. Calvetti, C. Tamagnini, and G. Viggiani. On the incremental behaviour of granular soils. In *Numerical Models in Geomechanics*, Swets & Zeitlinger, (2002), 3-9
- 25.F. Alonso-Marroquin and H. J. Herrmann. Ratcheting of granular materials. *Phys. Rev. Lett.*, 92(5), (2004), 054301.
- 26.P. A. Vermeer. A five-constant model unifying well established concepts. In *Constitutive Relations of soils*, Rotterdam, Balkema, (1984), 175–197.
- 27.R. Nova and D. Wood. A constitutive model for sand in triaxial compression. *Int. J. Num. Anal. Meth. Geomech.*, 3, (1979), 277–299.
- 28.F. Alonso-Marroquin and H.J. Herrmann. Investigation of the incremental response of soils using a discrete element model. *J. of Eng. Math.*, 52, (2005), 11–34.
- 29.Y. Kishino. On the incremental nonlinearity observed in a numerical model for granular media. *Italian Geotechnical Journal*, 3, (2003), 3–12.
- 30.F. Calvetti, G. Viggiani, and C. Tamagnini. Micromechanical inspection of constitutive modelling. In *Constitutive modelling and analysis of boundary value problems in Geotechnical Engineering*, Benevento, Hevelius Edizioni, (2003), 187–216.
- 31.F. Darve, E. Flavigny, and M. Meghachou. Yield surfaces and principle of superposition: revisit through incrementally non-linear constitutive relations. *International Journal of Plasticity*, 11(8), (1995), 927.

- 32.A. Pena, A. Lizcano, F. Alonso-Marroquin, and H. J. Herrmann. Biaxial test simulations using polygonal particles. *Int. J. Num. Anal. Meth. Geomech.* In press. (2007).
- 33.C. Goldenberg and I. Goldhirsch. Small and large scale granular statics. *Granular Matter*, 6, (2004) 97–96.
- 34.S. Roux and F. Radjai. On the state variables of the granular materials. In *Mechanics of a New Millenium*, Kluwer, Dordrecht, (2001), 181–196.
- 35.I. Vardoulakis. Rigid granular plasticity model and bifurcation in the triaxial test. *Acta Mechanica*, 49, (1983), 57–79.
- 36.F. Lekarp, A. Dawson, and U. Isacsson. Permanent strain response of unbound aggregates. *J. Transp. Engrg.*, 126(1), (2000), 76–82.
- 37.R. W. Sharp and J. R. Booker. Shakedown of pavements under moving surface loads. *Journal of Transportation Engineering*, 110, (1984), 1–14.
- 38.D. M. Wood. *Soil Mechanics-transient and cyclic loads*. John Wiley and Sons Ltd., Chichester, 1982.
- 39.G. Festag. Experimental investigation on sand under cyclic loading. In *Constitutive and Centrifuge Modelling: two Extremes*, Monte Verita, (2003), 269–277.
- 40.G. Festag. Experimentelle und numerische Untersuchungen zum Verhalten von granularen Materialien unter zyklischer Beanspruchung. Dissertation TU Darmstadt, 2003.
- 41.G. Gudehus. Ratcheting und DIN 1054. 10. Darmstadter Geotechnik-Kolloquium, 64, (2003), 159–162.
- 42.R. Garcia-Rojo, F. Alonso-Marroquin, and H. J. Herrmann. Characterization of the material response in granular ratcheting. *Phys. Rev. E*, 72, (2005), 041302.

- 43.T. Unger, J. Torok, J. Kertesz, and D. E. Wolf. Shear band formation in granular media as a variational problem. *Phys. Rev. Lett.*, 92(21), (2004), 214301.
- 44.I. Vardoulakis and J. Sulem. *Bifurcation analysis in geomechanics*. Blakie Academic & Professional, London, 1995.
- 45.F. Alonso-Marroqun, I. Vardoulakis, H. J. Herrmann, D. Weatherley, and P. Mora. Effect of rolling on dissipation in fault gouges. *Phys. Rev. E*, 74, (2006), 031306.
- 46.F. Nicot and F. Darve. A multiscale approach to granular materials. *Mech. mater.*, 37(9), (2005), 980–1006.